Journal of Hazardous Materials 172 (2009) 1111–1121

Contents lists available at ScienceDirect

Journal of Hazardous Materials

journal homepage: www.elsevier.com/locate/jhazmat

Biosorption of azo dyes from aqueous solution by glutaraldehyde-crosslinked chitosans

Arh-Hwang Chen*, Shin-Ming Chen

Department of Chemical and Materials Engineering, Southern Taiwan University, Tainan 710, Taiwan, ROC

ARTICLE INFO

Article history:
Received 1 April 2009
Received in revised form 1 July 2009
Accepted 27 July 2009
Available online 3 August 2009

Keywords:
Biosorption
Azo dye
Crosslinked chitosan microparticle
Competition
Desorption

ABSTRACT

The crosslinked chitosan microparticles prepared through homogeneous coupling reaction and microparticle formation using a sodium hydroxide solution showed the largest adsorbed amounts toward the RB5 and 3R dyes than those from the three other methods through heterogeneous coupling reaction and microparticle formation using sodium hydroxide or sodium tripolyphosphate solutions. The dynamical experimental study showed that the dye adsorption accurately followed the second-order adsorption process. The experimental isotherm data were analyzed using three isotherm models, namely, Langmuir, Freundlich, and Dubinin-Radushkevich. The results revealed that the adsorption behavior of the RB5 and 3R dyes on the microparticles fitted well with the Langmuir model. In addition, the mean adsorption energy (E) from the Dubinin-Radushkevich isotherm and the activation energy (E_a) from Arrhenius equation indicated that the adsorption process might be the dual nature of the process, physisorption and chemisorption, and was predominant on the chemisorption process The competitive adsorption showed that the adsorption of the 3R dye on the microparticles in the mixture solution was much more affected by the existence of the RB5 dye than the other way around. Furthermore, it was also found that the crosslinked chitosan microparticles can be regenerated and reused for dye adsorption.

1. Introduction

Dyes are widely used in various industries such as dyestuffs, textiles, leather, papers, plastics, and the like. Unfortunately, dyes that remain in waste effluents undergo chemical changes, consume dissolved oxygen, and destroy aquatic creatures. Moreover, these dyes may cause suspected carcinogenic and genotoxic effects. However, due to the large degree of aromatic rings present in the dye molecules, the treatment of wastewaters via a biological process is difficult and ineffective, resulting in their being discharged into the environment [1].

In this light, a wide range of conventional treatment processes including coagulation, precipitation, membrane filtration, oxidation, adsorption, and photodegradation have been utilized for removing dyes from wastewater [1–4]. Among all wastewater treatments, the adsorption process has been recognized to be an effective and economical procedure for the removal of dyes from industrial effluents. A large variety of adsorbent materials have been tested to remove dyes including activated carbon, which is one of the most widely used adsorbents because of its excellent adsorption capacity for organic pollutants. Because it is very expensive, low-cost biosorbent materials with high adsorption capacities have gained increasing attention in reducing the adsorbent dose and minimizing the disposal problem. In connection with this, special attention has been given to polysaccharides such as chitosan, which is a natural aminopolymer. Specifically, chitosan is a linear polycationic polymer containing 2-acetoamido-2-deoxy-β-D-glucopyranose and 2-amino-2-deoxy-β-D-glucopyranose residues. It has served as one of the most popular adsorbents for the removal of metal ions, dyes and proteins from an aqueous solution and has been widely used in waste treatment applications [5–11]. However, it is easily soluble in dilute organic acids, such as formic acid, acetic acid, and the like. The amino groups of chitosan are fully protonated at about pH 3.0, and the polymer chains with positive charges fall apart in the solution resulting in dissolution. Therefore, the crosslinking reaction with epichlorohydrin or glutaraldehyde and the chemical modification with glycidyl trimethyl ammonium chloride of raw chitosan have been used to improve the following: its chemical stability in any acid media, its resistance to biochemical and microbiological degradation, and its selectivity and capacity for the adsorption of metals and dyes from industrial effluents [12–17]. Although the crosslinking method may reduce the adsorption capacity of chitosan to remove dyes, it can enhance its resistance of chitosan against acids and chemicals. This may be attributed to the extent of crosslinking and the decreased amount of the amino

* Corresponding author. Tel.: +886 6 2533131x6937; fax: +886 6 2432846.
E-mail address: chenah@ms12.hinet.net (A.-H. Chen).

0304-3894/$ – see front matter © 2009 Elsevier B.V. All rights reserved.
doi:10.1016/j.jhazmat.2009.07.104

Nomenclature

A	Arrhenius factor
$A_{\lambda i}$	absorbance of dye solution at wavelength λi
b_F	Freundlich adsorption intensity
C_{dye}	concentration of dye solution (M)
C_e	equilibrium concentration of dye (mg/mL)
C_f	final concentration of dye (mg/mL)
C_i	initial concentration of dye (mg/mL)
E	mean adsorption energy (kJ/mol)
E_a	activation energy (kJ/mol)
K	Dubinin-Radushkevich constant (kJ^2/mol^2)
K_C	equilibrium constant
K_F	Freundlich maximum adsorption capacity of dye (mg/g)
K_L	Langmuir adsorption equilibrium constant
L	cell width (1 cm)
Q	adsorption capacity of dye (mg/g)
Q_{DR}	Dubinin-Radushkevich maximum adsorption capacity of dye (mg/g)
Q_e	adsorption capacity of dye (mg/g) at equilibrium
Q_m	Langmuir maximum adsorption capacity of dye (mg/g)
Q_t	adsorption capacity of dye (mg/g) at a given time t
R	gas constant (8.314 J/(K mol))
R^2	correlation coefficient
S.D.	standard deviation
T	absolute temperature (K)
V	volume of dye solution (mL)
W	weight of the crosslinked chitosan used (g)
ΔG°	standard free energy change (kJ/mol)
ΔH°	standard enthalpy change (kJ/mol)
ΔS°	standard entropy change (J/mol K)
ε	Polanyi potential
$\varepsilon_{\lambda i,dye}$	molar absorptivity of dye (L/(cm mol))

group, which is expected to play a great part in the adsorption process.

In the present study, the crosslinked chitosan microparticles were prepared from four methods based on the formation of microparticles in the sodium hydroxide and sodium tripolyphosphate solutions, as well as on the sequence of crosslinking reaction with glutaraldehyde. The crosslinked chitosan microparticles were then characterized using FTIR, solid state ^{13}C NMR, and TGA. Afterwards, they were used for adsorption of two azo dyes, namely, Remazol Black 5 (RB5) and Remazol Brilliant Orange 3R (3R), in an aqueous solution. Furthermore, pH influence, kinetics, equilibrium, thermodynamics, competition and reuse were examined to gain better comparison of the experimental results. This information would be useful for further applications in the treatment of waste effluents from the dye industry.

2. Materials and methods

2.1. Chemicals

Chitosan used in this study was purchased from Sigma–Aldrich Co., USA. It was then hydrolyzed with sodium hydroxide to give it a deacetylation percentage of approximately 90% following the FTIR methods. The average molecular weight of was 690,000 as measured through the viscometric method. The two azo dyes, namely, Remazol Black 5 (RB5; purity 55%; Mw = 991.82 g/mol; λ_{max} = 597 nm) and Remazol Brilliant Orange 3R (3R; purity 50%; Mw = 617.54 g/mol; λ_{max} = 494 nm), were purchased from Sigma–Aldrich Co., USA. The structures of the two azo dyes are displayed in Fig. 1. Meanwhile, glutaraldehyde and sodium tripolyphosphate with 50% and 85% purity, respectively, were purchased from Acros Organics, Belgium. All the reagents were used without undergoing further purification.

2.2. Methods for preparation

The preparation of the glutaraldehyde-crosslinked chitosan microparticles was involved three steps: chitosan dissolution, formation of microparticles and reaction of crosslinking. In this study, the microparticles were prepared using the methods described below.

(a) A-method: A solution of chitosan was prepared with 0.125 g of chitosan dissolved into a 25 mL aqueous solution of acetic acid (1%, v/v). A 12.5 mL aqueous solution of glutaraldehyde was then added dropwise, after which the mixture was stirred for 1 h at room temperature. Subsequently, the chitosan solution was slowly dropped through a syringe into 25 mL of 0.5 M sodium hydroxide solution with mechanical stirring to form the microparticle precipitates. The precipitates were filtered out and washed with distilled water and acetone. They were then dried inside a vacuum oven at 50 °C for 8 h. The resulting materials were sieved to collect particles with three different diameter sizes: 149–250, 250–500, and 500–1000 μm.

(b) B-method: A chitosan solution was prepared as in (a). Subsequently, it was slowly dropped through a syringe into 25 mL of a 1% sodium tripolyphosphate solution with mechanical stirring to form the microparticle precipitates. These were filtered out and washed with distilled water and acetone. They were then dried inside in a vacuum oven at 50 °C for 8 h. The resulting materials were sieved to collect particles with a diameter between 149 and 250 μm.

(c) C-method: A solution of chitosan was prepared as in (a). Subsequently, it was slowly dropped through a syringe into 25 mL of 0.5 M sodium hydroxide solution with mechanical stirring to form the microparticle precipitates. The precipitates were filtered out and washed with distilled water. Then, the microparticle precipitates were suspended in 50 mL of glutaraldehyde solution, after which the mixture was stirred for 6 h at room temperature. The crosslinked chitosan microparticles were filtered out and washed with distilled water and acetone. They were the dried inside in a vacuum oven at 50 °C for 8 h. The resulting materials were sieved to collect particles with a diameter between 149 and 250 μm.

(d) D-method: A chitosan solution was prepared as in (a). Subsequently, it was slowly dropped through a syringe into 25 mL of 1% sodium tripolyphosphate solution with mechanical stirring to form the microparticle precipitates. The precipitates were filtered out and washed with distilled water. Then, the microparticle precipitates were suspended in 50 mL of glutaraldehyde solution, after which the mixture was stirred for 6 h at room temperature. The crosslinked chitosan microparticles were filtered out and washed with distilled water and acetone. They were then dried inside in a vacuum oven at 50 °C for 8 h. The resulting materials were sieved to collect particles with a diameter between 149 and 250 μm.

2.3. Adsorption of azo dyes

The microparticles that were prepared from four methods with different molar ratios of GLA/chitosan, were studied to determine the adsorption capacities of the two azo dyes. This process was car-

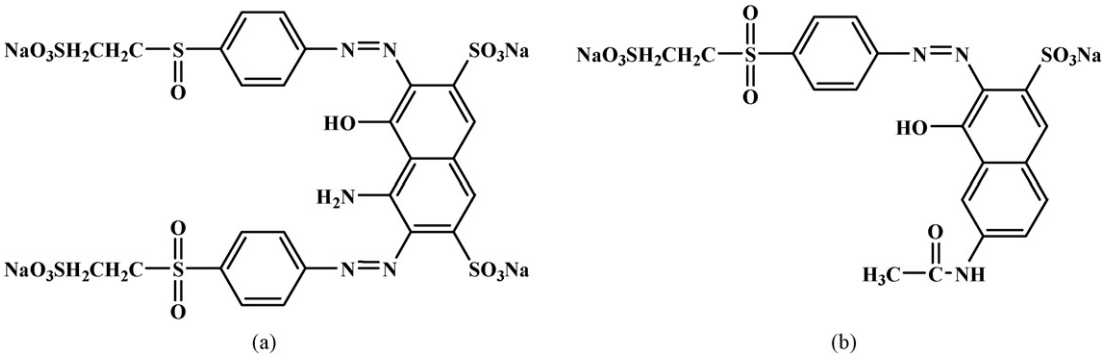

Fig. 1. The structures of (a) Remazol Black 5 and (b) Remazol Brilliant Orange 3R.

ried out by adding 10 mg of each kind of microparticles into a 10 mL of 2.0 mg/mL dye solution at pH 3.0 while stirring at 30 °C for 168 h. The solution was filtered and adjusted to a pH level of 6.0 using a hydrochloric acid solution or sodium hydroxide solution. The dye concentration was measured using an ultraviolet spectrophotometer, Shimadzu UV-2401 PC, while the adsorption capacity (Q) (mg/g) was calculated through Eq. (1):

$$Q = (C_i - C_f)\frac{V}{W} \quad (1)$$

2.4. Characterization of the crosslinked chitosans

The microparticles were determined through the Fourier transform infrared spectra (FTIR) using a Perkin Elmer Spectrum One FTIR spectrometer. Meanwhile, the solid state ^{13}C nuclear magnetic resonance spectra of the materials were measured on a Brucker Advance 400 NMR spectrometer. The thermogravimetric analysis (TGA) curves were performed on a Perkin Elmer TGA 7 analyzer.

2.5. Batch kinetics

The adsorption kinetics of the two azo dyes on the A-method microparticles was carried out in a batch process. The variable parameters were studied, including the initial concentrations of dyes as well as temperatures. In each test, 10 mg of the A-method microparticles was conducted in 10 mL of aqueous solution of each azo dye with a known concentration. Whenever necessary, the pH value was adjusted with dilute sodium hydroxide or hydrochloric acid solutions. Afterwards, 0.1 mL aliquots of the solution at different time intervals were filtered, adjusted to pH 6.0 and then, diluted to 10 mL. The concentrations of azo dyes were then measured using an ultraviolet spectrophotometer. The amount of adsorption was calculated using Eq. (1).

2.6. Batch equilibrium

The equilibrium studies were carried out by suspending 10 mg of each A-method microparticles with three different diameter sizes in 10 mL of initial dye concentrations within the range of 0.5–3.0 mg/mL at pH 3.0 and with stirring for 168 h at 30 °C. The solutions were filtered, adjusted to pH 6.0, and then diluted to 10 mL. The concentrations of the azo dyes were measured using an ultraviolet spectrophotometer. According to Eq. (1), the amount of adsorption was then calculated based on the differences of the concentration in an aqueous solution (10 mL) before and after the adsorption, as well as on the weight of the microparticles (0.010 g) themselves.

3. Results and discussion

3.1. Adsorption

The crosslinked chitosan microparticles were utilized in order to determine the adsorption of the RB5 and 3R dyes. As shown in Fig. 2, they were found to have the maximum adsorption capacities toward the RB5 and 3R dyes at the 0.25 molar ratio of GLA/chitosan. The adsorption capacities of the RB5 and 3R dyes revealed the following order: A-method > B-method > C-method > D-method. In the crosslinking step, the homogeneous reaction of chitosan being dissolved in aqueous acetic acid seemed to have easily reacted with glutaraldehyde than the heterogeneous reaction of chitosan microparticles being suspended in an aqueous glutaraldehyde solution. This may be attributed to the crosslinking reaction that only occurred at the surface of the microparticles during the heterogeneous reaction. Additionally, in the microparticles formation step,

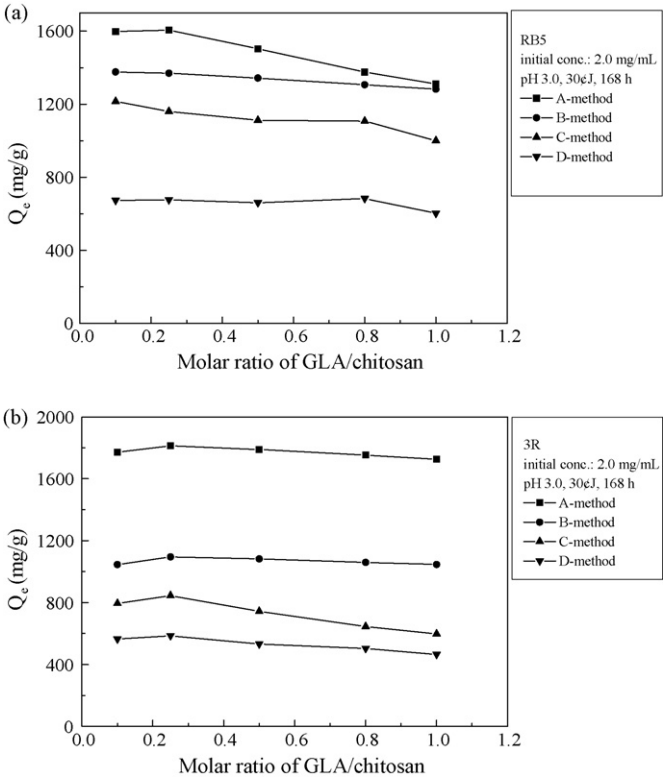

Fig. 2. Adsorption capacities of two azo dyes: (a) RB5 and (b) 3R on the crosslinked chitosans (diameter: 149–250 μm) prepared from four methods with different molar ratios of GLA/chitosan.

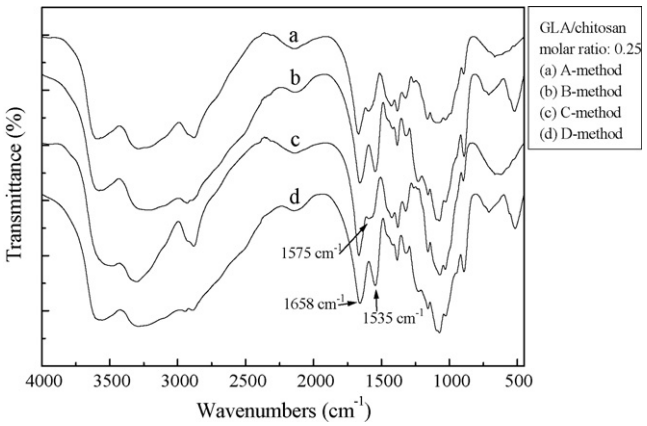

Fig. 3. FTIR spectra of the crosslinked chitosans prepared from (a) A-method, (b) B-method, (c) C-method and (d) D-method with 0.25 molar ratio of GLA/chitosan.

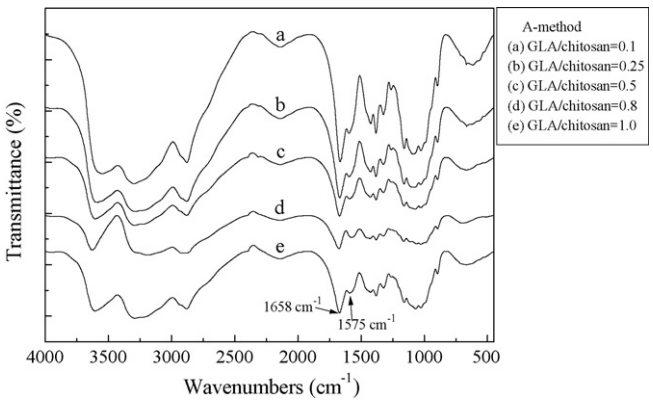

Fig. 4. FTIR spectra of the crosslinked chitosans prepared from A-method with different molar ratios of GLA/chitosan.

sodium tripolyphosphate may have made the chitosan microparticles more rigid than sodium hydroxide because of the ionic attraction between tripolyphosphate ions ($P_3O_{10}^{5-}$) and the protonated amino groups ($-NH_3^+$) of chitosan in an acid solution [18]. However, the microparticles formed using sodium tripolyphosphate should have a lower adsorption of RB5 and 3R dyes than those formed using sodium hydroxide. This could be attributed to the anionic repulsion between the microparticles with tripolyphosphate ions and the dyes with sulfonate ions. Therefore, the crosslinked chitosan microparticles from the A-method had the largest adsorption capacities toward the RB5 and 3R dyes than those from the three other methods.

3.2. Characterization

Fig. 3 shows that the crosslinked chitosan microparticles prepared from the above mentioned methods were characterized using the Fourier transform infrared spectra (FTIR). As can be seen, the microparticles prepared from the A- and C-methods showed an absorption peak for imine C=N and amide C=O stretching vibrations at 1658 cm^{-1}, and another absorption peak for amide N–H bending vibration at 1575 cm^{-1} [19]. However, the microparticles prepared from the B- and D-methods had an intense absorption peak of 1535 cm^{-1}, which accounted for the tripolyphosphate ions ($P_3O_{10}^{5-}$). In preparation from the A-method, the FTIR spectra of the microparticles with different molar ratios of GLA/chitosan are shown in Fig. 4. From the results, we can see that the absorbance ratios of A_{1658}/A_{1575} for the crosslinked chitosan microparticles becomes higher than that of the native chitosan, as the crosslinking degree increases via the formation of Schiff's base linkage. The degrees of crosslinking were 6.1, 6.9, 12.1, 15.2, and 15.8%, respectively, with 0.1, 0.25, 0.5, 0.8 and 1.0 molar ratios of GLA/chitosan used in the preparation. Meanwhile, the solid state ^{13}C NMR spectra of the microparticles prepared from the A-method with 0.25 molar ratio of GLA/chitosan appeared to have five peaks at 29.3, 41.1, 46.7, 91.7, and 97.6 ppm due to the exiting of $-N{=}C(CH_2)_3C{=}N-$ linkage between two chitosan molecules in comparison with chi-

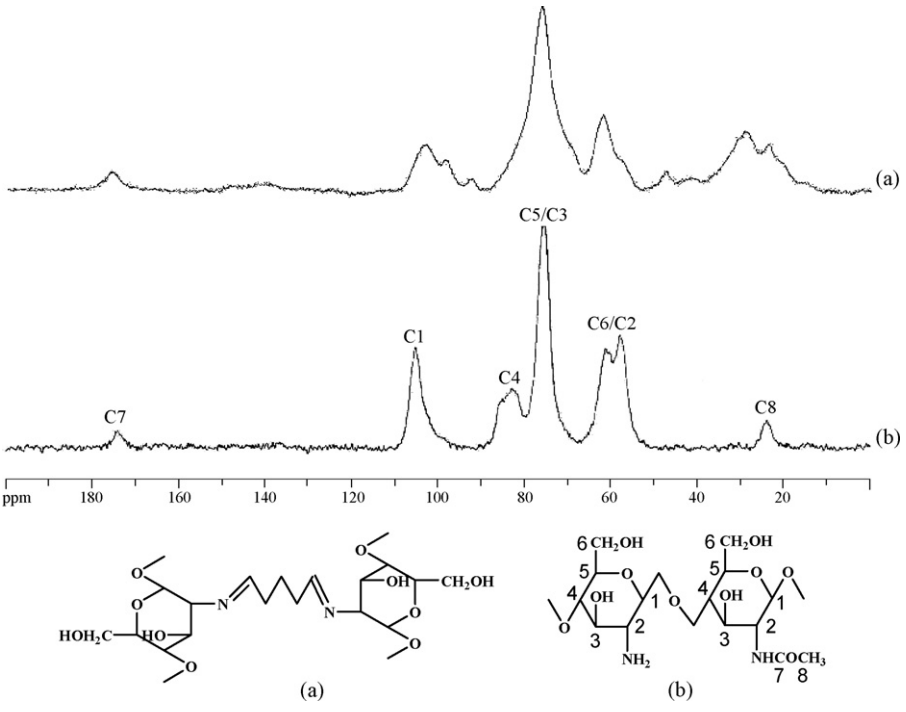

Fig. 5. Solid state ^{13}C NMR spectra of (a) the crosslinked chitosan prepared from A-method (diameter: 149–250 μm) with 0.25 molar ratio of GLA/chitosan and (b) the chitosan with a partial acetylation.

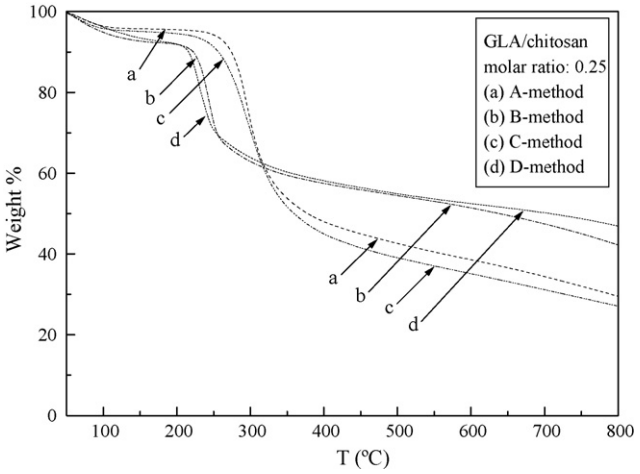

Fig. 6. TGA curves of the crosslinked chitosans (diameter: 149–250 μm) prepared from (a) A-method, (b) B-method, (c) C-method and (d) D-method with 0.25 molar ratio of GLA/chitosan.

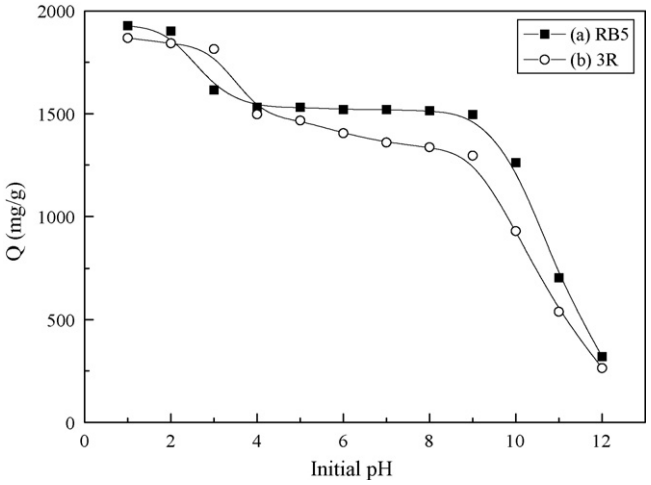

Fig. 8. The effect of pH for adsorption capacities of (a) RB5 and (b) 3R on the A-method microparticles (diameter: 149–250 μm) at 2.0 mg/mL initial concentration of azo dyes and 30 °C with different pHs.

tosan (Fig. 5). The thermal decomposition temperatures (T_d) of the microparticles prepared from the A-method (273.5 °C) and the C-method (260.9 °C) were found to be higher than those prepared from the B-method (224.3 °C) and the D-method (218.0 °C) (Fig. 6). These results indicated that the microparticles formed from sodium tripolyphosphate solution were more easily decomposed than those formed from the sodium hydroxide solution. This could be attributed to the decomposition of tripolyphosphate into phosphoric acid. However, the thermal decomposition temperatures (T_d) of the microparticles prepared from the A-method with 0.1, 0.25, 0.5, 0.8, and 1.0 molar ratios of GLA/chitosan (274.2, 273.5, 268.9, 260.8, and 254.4 °C, respectively) appeared to have decreased a little along with increasing molar ratio of GLA/chitosan. This could be due to the loss of glutaraldehyde moiety at higher molar ratio of GLA/chitosan (Fig. 7). Therefore, the crosslinked chitosan microparticles had more thermal stability from the preparation carried out through the homogenous coupling reaction and the microparticles formation from sodium hydroxide solution.

3.3. Initial pH influence

The effects of initial pH on the adsorption capacities of the RB5 and 3R dyes on the A-method microparticles were shown in Fig. 8.

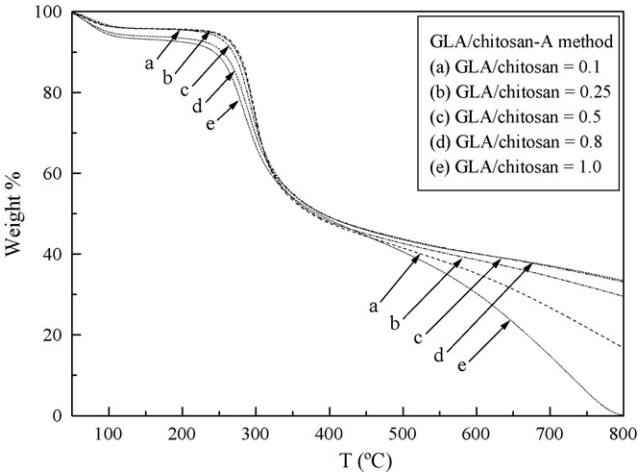

Fig. 7. TGA curves of the crosslinked chitosans (diameter: 149–250 μm) prepared from A-method with different molar ratios of GLA/chitosan.

The pH values were monitored before and after the adsorption of dyes with only pH differences from 0.1 to 0.2. As can be seen, the adsorption capacities of these two dyes decreased with the increase of the initial pH of solution. Their adsorption capacities changed slightly from pH 1.0 to pH 9.0, then, decreased largely when the pH value exceeded 9.0. The adsorption capacities of the RB5 and 3R dyes were 1927 and 1868 mg/g, respectively, at initial pH 1.0. These then decreased to 319 and 264 mg/g, respectively, at initial pH 12.0. At a lower pH solution, more protons will be available to protonate the amino groups of chitosan molecules to form $-NH_3^+$ groups; this increases electrostatic attraction between the anionic group ($-SO_3^-$) of the dye and the protonated amino group ($-NH_3^+$) of chitosan, causing an increase in dye adsorption [20]. However, a lower dye adsorption at a higher pH solution may be due to the abundance of hydroxide ions (OH^-) and the ionic repulsion occurring between the anionic dye molecules and the negatively charged surface of the chitosan microparticles.

3.4. Adsorption kinetics

Fig. 9 showed the adsorption kinetics of the RB5 and 3R dyes on the A-method microparticles at pH 3.0 and 30 °C, with three different initial concentrations of dyes. As the initial dye concentrations of the RB5 and 3R dyes changed from 1.5 to 2.5 mg/mL, the adsorption capacities then increased from 1373 to 1664 mg/g for the RB5 dye, and from 1340 to 1952 mg/g for the 3R dye. However, along with an increase in the initial dye concentration from 1.5 to 2.5 mg/mL, their dye removal efficiencies decreased from 100 to 72.7% (RB5 dye) and from 100 to 87.4% (3R dye). This might be ascribed to the fact that the ratio of the initial moles of dye compared to the available surface area was low at the low initial concentration; therefore, the subsequent fractional adsorption became independent of the initial concentration; however, at the high concentration, the available adsorption sites were fewer than the moles of the dye present; hence, the percentage of dye removal was dependent on the initial dye concentration [21].

Fig. 10 presented the effects of temperature on the dye adsorption capabilities of the RB5 and 3R dyes on the A-method microparticles at a 2.0 mg/mL initial dye concentration and a pH level 3.0. During the tests, an increase in the temperature led to an increase in initial adsorption rate, although the adsorption capacities at 120 h were close to each other. In addition, the adsorption capacity showed different trends at different temperatures before and after the equilibrium time. Before the equilibrium time, the

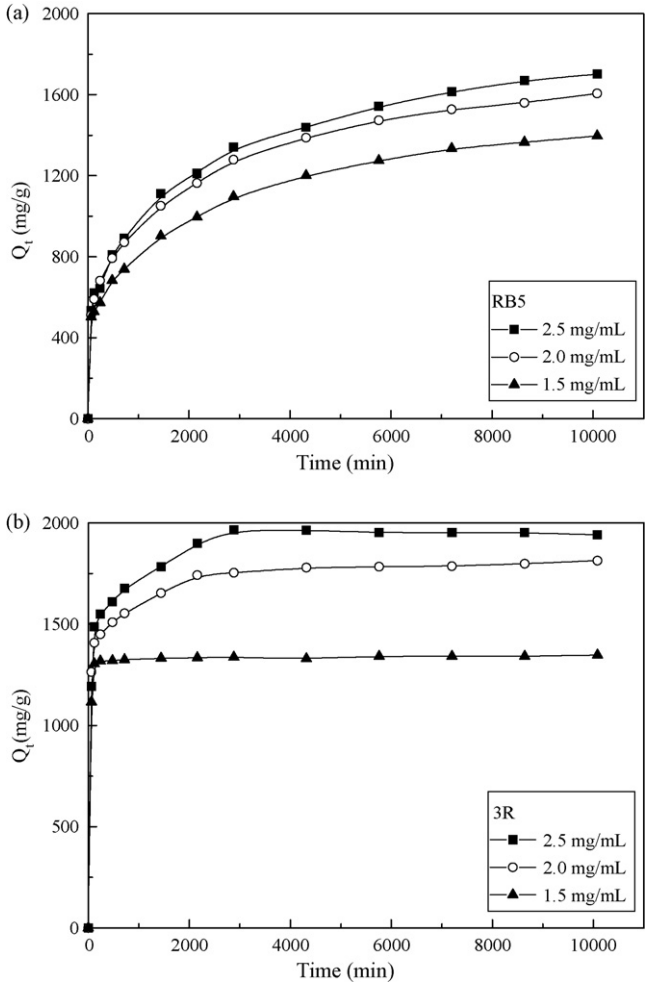

Fig. 9. Adsorption kinetics of (a) RB5 and (b) 3R on the A-method microparticles (diameter: 149–250 μm) at pH 3.0 and 30 °C with different initial concentrations of azo dyes.

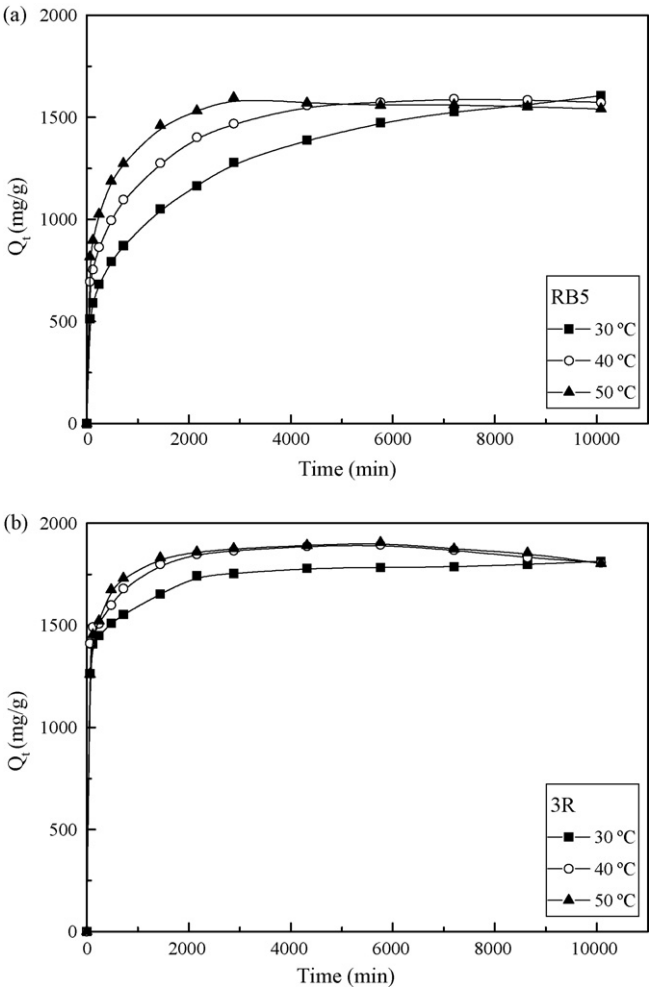

Fig. 10. Adsorption kinetics of (a) RB5 and (b) 3R on the A-method microparticles (diameter: 149–250 μm) at 2.0 mg/mL initial concentration of azo dyes and pH 3.0 with different temperatures.

adsorption rate and capacity increased along with an increase in the temperature, revealing a kinetically controlled process. After the equilibrium time, the decrease of adsorption along with the increasing temperature indicated that the adsorption of dye on the microparticles was controlled by an exothermic process [13]. However, the results showed that the adsorption capacities of the RB5 and 3R dyes on the microparticles at 168 h decreased only at 2.1, 4.1, 0.2, and 0.6%, respectively, at 40 and 50 °C than those at 30 °C. Hence, the temperature variations of normal wastewater did not significantly affect the overall removal performance of these dyes from the wastewater.

In order to investigate the mechanism of dye adsorption on the microparticles, the dynamical experimental data were applied to the first-order and the second-order kinetics.

The first-order kinetics is represented by the Eq. (2):

$$\ln(Q_e - Q_t) = \ln Q_e - k_1 t \tag{2}$$

The plot of $\ln(Q_e - Q_t)$ versus t gives a straight line with a slope of $-k_1$ and an intercept of $\ln Q_e$.

The second-order kinetics is expressed as Eq. (3):

$$\frac{t}{Q_t} = \frac{1}{k_2 Q_e^2} + \frac{t}{Q_e} \tag{3}$$

Table 1
Comparison of the first- and second-order adsorption rate constants, experimental and calculated Q_e values with different initial concentrations of RB5 dye and with different temperatures on the A-method microparticles (diameter: 149–250 μm).

Parameter	Q_e (mg/g) (S.D.)	First-order kinetic model			Second-order kinetic model		
		k_1 ($\times 10^{-3}$) (min^{-1}) (S.D.)	$Q_{e,cal}$ (mg/g) (S.D.)	R^2	k_2 ($\times 10^{-6}$) (g/(mg min)) (S.D.)	$Q_{e,cal}$ (mg/g) (S.D.)	R^2
Initial dye concentration (mg/mL), time = 168 h (pH 3.0, 30 °C)							
1.5	1396.0 (32.4)	0.37 (0.01)	893.8 (17.4)	0.9932	1.23 (0.06)	1428.9 (28.8)	0.9937
2.0	1606.1 (28.8)	0.36 (0.03)	994.4 (47.5)	0.9962	1.12 (0.06)	1639.8 (38.0)	0.9947
2.5	1701.9 (52.6)	0.40 (0.08)	1163.8 (177.3)	0.9712	0.96 (0.11)	1756.5 (87.1)	0.9933
Temperature (°C), time = 168 h (2.0 mg/mL, pH 3.0)							
30	1606.1 (28.8)	0.36 (0.03)	994.4 (47.5)	0.9962	1.12 (0.06)	1639.8 (38.0)	0.9947
40	1573.3 (1.0)	0.89 (0.10)	882.6 (103.4)	0.9335	2.50 (0.20)	1626.1 (18.7)	0.9991
50	1540.9 (10.3)	0.87 (0.03)	256.0 (80.0)	0.7298	7.70 (1.16)	1574.9 (17.5)	0.9996

The plot of t/Q_t versus t gives a straight line with a slope of $1/Q_e$ and an intercept of $1/(k_2Q_e^2)$.

Tables 1 and 2 listed the results of rate constants for the RB5 and 3R dyes with different initial dye concentrations and with different temperatures on the microparticles by the first-order and the second-order kinetics. The correlation coefficients, R^2, from the second-order adsorption kinetics were higher than those from the first-order kinetics. At the same time, the calculated equilibrium adsorption capacities, $Q_{e,cal}$, from the second-order adsorption kinetics fitted well with the experimental data. These suggested that the second-order adsorption mechanism was predominant and that the overall rate of the process of dye adsorption appeared to be controlled by a chemical process. This could be ascribed to the fact that the rate-determining step might have involved valency force through the sharing of electrons between dye anions and adsorbent [12].

3.5. Adsorption equilibrium

Fig. 11 showed the adsorption isotherms of the two dyes on different sizes of the A-method microparticles at pH 3.0 and 30 °C with different equilibrium dye concentrations. The equilibrium adsorption capacity of the dye, Q_e, increased with the increase in dye concentration. At the same time, its adsorption capacity decreased slightly with increasing diameter of the microparticle. This suggested that the adsorption took place mainly on the outer surface of the microparticle due to steric hindrance of the dye molecules. The dye adsorption was increased with a decrease in the particle size given that the effective surface area was higher for the same mass of smaller particles. However, the equilibrium adsorption capacity of the 3R dye (Q_e) was much higher that that of the RB5 dye as the equilibrium concentration of dye, C_e, became greater than 0.016 mM. This may be due to the fact that the molecular size of the 3R dye is much smaller than that of the RB5 dye (Fig. 1), and that more molecules of the smaller 3R dye can be adsorbed by the per unit weight of the adsorbent.

The biosorption isotherms for the RB5 and 3R dyes on the different sizes of the microparticles were studied using three isotherm models, namely, Langmuir, Freundlich, and Dubinin-Radushkevich.

The Langmuir isotherm equation for monolayer adsorption on to a surface with a finite number of identical sites is represented by the Eq. (4) [22]:

$$\frac{C_e}{Q_e} = \frac{C_e}{Q_m} + \frac{1}{Q_m K_L} \quad (4)$$

The plot of C_e/Q_e against C_e gives a straight line with a slope of $1/Q_m$ and an intercept of $1/(Q_mK_L)$.

The Freundlich isotherm equation for heterogeneous surfaces of multilayer adsorption is described by the Eq. (5) [23]:

$$\ln Q_e = b_F \ln C_e + \ln K_F \quad (5)$$

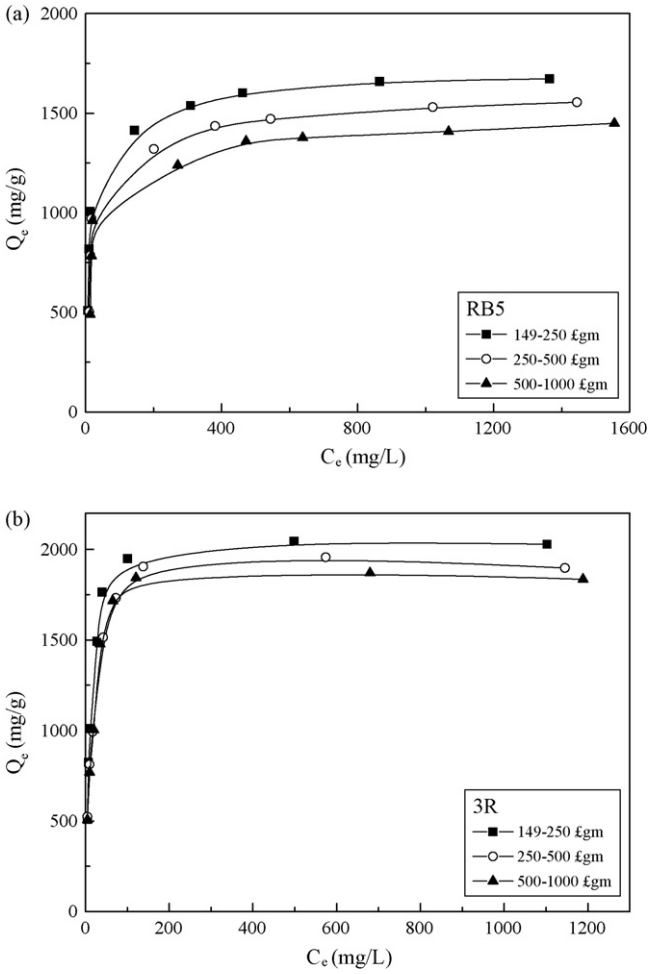

Fig. 11. Equilibrium adsorption of (a) RB5 and (b) 3R on different sizes of the A-method microparticles at pH 3.0 and 30 °C with different initial concentrations of azo dyes.

Freundlich constants, K_F and b_F, can calculated from a linear plot of $\ln Q_e$ versus $\ln C_e$.

The Dubinin-Radushkevich isotherm equation used to distinguish between physical and chemical adsorption is given by Eq. (6) [24]:

$$\ln Q_e = K_\varepsilon^2 + \ln Q_{DR} \quad (6)$$

Polanyi potential (ε) is given as the Eq. (7):

$$\varepsilon = RT \ln\left(1 + \frac{1}{C_e}\right) \quad (7)$$

Table 2
Comparison of the first- and second-order adsorption rate constants, experimental and calculated Q_e values with different initial concentrations of 3R dye and with different temperatures on the A-method microparticles (diameter: 149–250 μm).

Parameter	Q_e (mg/g) (S.D.)	First-order kinetic model			Second-order kinetic model		
		k_1 ($\times10^{-3}$) (min^{-1}) (S.D.)	$Q_{e,cal}$ (mg/g) (S.D.)	R^2	k_2 ($\times10^{-5}$) (g/(mg min)) (S.D.)	$Q_{e,cal}$ (mg/g) (S.D.)	R^2
Initial dye concentration (mg/mL), time = 168 h (pH 3.0, 30 °C)							
1.5	1346.7 (9.3)	0.30 (0.24)	39.3 (26.7)	0.4454	5.64 (2.09)	1342.3 (12.7)	1.0000
2.0	1813.6 (1.4)	0.41 (0.07)	322.7 (77.6)	0.8520	0.65 (0.16)	1818.2 (0.1)	0.9998
2.5	1942.1 (14.3)	0.88 (0.03)	304.4 (45.7)	0.7838	0.76 (0.13)	1960.8 (0.1)	0.9998
Temperature (°C), time = 168 h (2.0 mg/mL, pH 3.0)							
30	1813.6 (1.4)	0.41 (0.07)	322.7 (77.6)	0.8520	0.65 (0.16)	1818.2 (0.1)	0.9998
40	1807.2 (0.6)	0.74 (0.04)	92.9 (27.3)	0.6101	6.47 (3.42)	1851.9 (0.1)	0.9993
50	1803.4 (2.0)	0.70 (0.00)	69.0 (1.0)	0.5504	46.97 (12.87)	1851.9 (0.1)	0.9991

Table 3
Langmuir, Freundlich and Dubinin-Radushkevich isotherm parameters for RB5 dye on different particle sizes of the A-method microparticles at pH 3.0 and 30 °C.

	Particle size (μm)		
	149–250	250–500	500–1000
Langmuir isotherm			
Q_m (mg/g) (S.D.)	1680.8 (19.9)	1574.9 (17.5)	1459.9 (15.0)
K_L (L/mg) (S.D.)	0.0531 (0.0071)	0.0406 (0.0044)	0.0366 (0.0088)
R^2	0.9997	0.9994	0.9991
Freundlich isotherm			
K_F (mg/g) (S.D.)	494.1 (7.3)	457.7 (6.3)	440.7 (3.8)
b_F (S.D.)	0.1868 (0.0025)	0.1818 (0.0003)	0.1732 (0.0023)
R^2	0.8445	0.8313	0.7928
Dubinin-Radushkevich isotherm			
Q_{DR} (mg/g) (S.D.)	2868.1 (23.3)	2574.3 (48.7)	2309.0 (32.5)
K ($\times 10^{-8}$ J^2/mol^2) (S.D.)	−0.160 (0.002)	−0.159 (0.001)	−0.154 (0.002)
E (kJ/mol) (S.D.)	17.71 (0.11)	17.76 (0.04)	18.05 (0.13)
R^2	0.8735	0.8545	0.8115

Table 4
Langmuir, Freundlich and Dubinin-Radushkevich isotherm parameters for 3R dye on different particle sizes of the A-method microparticles at pH 3.0 and 30 °C.

	Particle size (μm)		
	149–250	250–500	500–1000
Langmuir isotherm			
Q_m (mg/g) (S.D.)	2041.6 (58.9)	1923.8 (52.33)	1852.4 (48.5)
K_L (L/mg) (S.D.)	0.1121 (0.0170)	0.1102 (0.0010)	0.1125 (0.0150)
R^2	0.9998	0.9995	0.9997
Freundlich isotherm			
K_F (mg/g) (S.D.)	572.1 (0.4)	516.7 (23.5)	518.7 (34.7)
b_F (S.D.)	0.2176 (0.0054)	0.2232 (0.0017)	0.2158 (0.0140)
R^2	0.7238	0.7810	0.7401
Dubinin-Radushkevich isotherm			
Q_{DR} (mg/g) (S.D.)	4228.9 (288.3)	4022.0 (149.5)	3837.4 (240.2)
K ($\times 10^{-8}$ J^2/mol^2) (S.D.)	−0.196 (0.008)	−0.203 (0.001)	−0.199 (0.013)
E (kJ/mol) (S.D.)	15.98 (0.34)	15.71 (0.03)	15.86 (0.51)
R^2	0.7869	0.8473	0.8140

The plot of ln Q_e versus ε^2 gives a straight line with a slope of K and an intercept of ln Q_{DR}. The Dubinin-Radushkevich constant can give the valuable information regarding the mean energy of adsorption by the Eq. (8):

$$E = (-2K)^{-1/2} \quad (8)$$

The adsorption isotherm equations for the RB5 and 3R dyes, according to these three isotherms, were summarized in Tables 3 and 4. In comparing the linear correlation coefficients listed in Tables 3 and 4, it could be concluded that the adsorptions of the two dyes on the different sizes of the microparticles, fitted well the Langmuir isotherm equation under the concentration range studied. Meanwhile, from the Dubinnin-Radushkevich isotherm, the mean adsorption energy (E) involved the transfer of the free energy of one mole of solute from infinity (in solution) to the adsorbent's surface. The adsorption behavior might have predicted the physical adsorption in the range of 1–8 kJ/mol of the mean adsorption energy, and the chemical adsorption in more than 8 kJ/mol of the mean adsorption energy [25,26]. The mean adsorption ener-

Table 5
Comparison of the maximum monolayer adsorption capacity (Q_{max}) of some azo dyes on various adsorbents.

Azo dye	Adsorbent and method of preparation	Q_{max} (mg/g)	Reference
Remazol Black 5	GLA-crosslinked chitosan, A-method	1680	This work
Remazol Brilliant Orange 3R	GLA-crosslinked chitosan, A-method	2041	This work
Reactive Red 189	ECH-crosslinked chitosan, heterogeneous coupling, using NaOH	1642–1936	[12]
Reactive Red 189	ECH-crosslinked chitosan, heterogeneous coupling, using TPP	1802–1840	[13]
Reactive Red 2	ECH-crosslinked chitosan, heterogeneous coupling, using TPP	2422	[15]
Reactive Yellow 2	ECH-crosslinked chitosan, heterogeneous coupling, using TPP	2436	[15]
Reactive Yellow 86	ECH-crosslinked chitosan, heterogeneous coupling, using TPP	1911	[15]
Acid Orange 12	ECH-crosslinked chitosan, heterogeneous coupling, using TPP	1954	[15]
Acid Red 14	ECH-crosslinked chitosan, heterogeneous coupling, using TPP	1940	[15]
Acid Orange 7	ECH-crosslinked chitosan, heterogeneous coupling, using TPP	1940	[15]
Direct Red 81	ECH-crosslinked chitosan, heterogeneous coupling, using TPP	2383	[15]
Metanil Yellow	ECH-crosslinked chitosan, heterogeneous coupling, using TPP	1337	[16]
Remazol Brilliant Orange 3R	GLA-crosslinked quaternary chitosan, heterogeneous coupling	1060	[17]
Reactive Black 5	Acid-treated biomass of brown seaweed Laminaria sp.	102	[21]
Reactive Black 5	Chitosan/amino resin and chitosan bearing both amine and quaternary ammonium chloride moieties	625–932	[27]

Note: The maximum monolayer adsorption capacity (Q_{max}) is obtained from Langmuir isotherm equation.

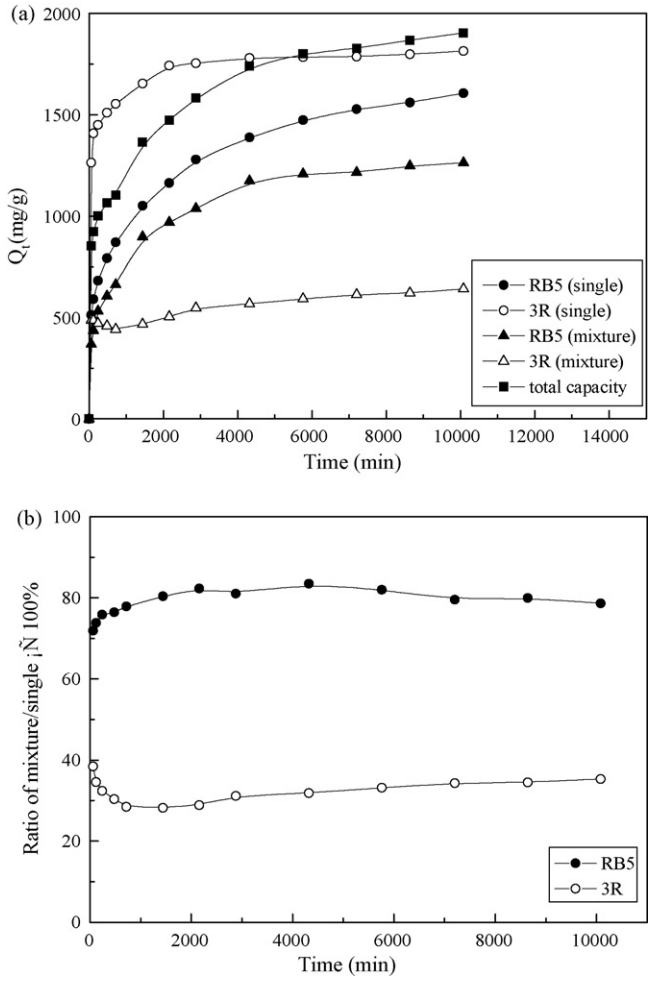

Fig. 12. (a) Absorption kinetics of the single and the mixture of azo dyes: RB5 and 3R, on the A-method microparticles (diameter: 149–250 μm) in 2.0 mM initial concentration of each dye at pH 3.0 and 30 °C. (b) The ratio of the adsorption capacity between the mixture solution and the single dye solution.

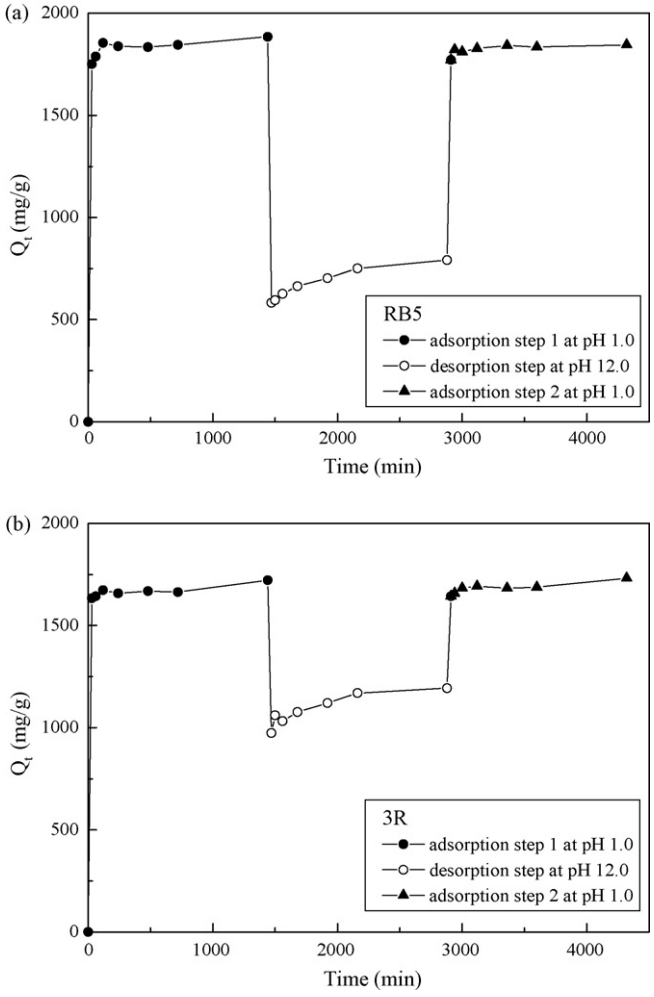

Fig. 13. Adsorption and desorption of (a) RB5 and (b) 3R on the A-method microparticles (diameter: 149–250 μm) at 2.0 mg/mL initial concentration of azo dyes and 30 °C with three steps: adsorption step 1 at pH 1.0, desorption step 2 at pH 12.0 and adsorption step 3 at pH 1.0.

gies (E) of the RB5 and 3R dyes, from 17.71 to 18.05 and from 15.71 to 15.98 kJ/mol, respectively, indicated that the adsorptions were predominant on the chemisorption process. Table 5 listed the comparison of maximum monolayer adsorption capacity (Q_{max}) of some azo dyes on various adsorbents. The data demonstrated that the microparticles in this work had relatively high adsorption capacities of the RB5 and 3R dyes.

3.6. Adsorption thermodynamics

The dependence of Langmuir adsorption equilibrium constant (K_L) with temperature was used to predict the thermodynamic parameters associated with the adsorption process. According to van't Hoff equation, the standard Gibbs free energy change (ΔG°), standard enthalpy change (ΔH°) and standard entropy change (ΔS°) were determined using the Eqs. (9) and (10) [27–29]:

$$\ln K_L = -\frac{\Delta H^\circ}{RT} + \frac{\Delta S^\circ}{R} \quad (9)$$

$$\Delta G^\circ = \Delta H^\circ - T\Delta S^\circ \quad (10)$$

By plotting a graph of $\ln K_L$ versus $1/T$, the values of ΔH° and ΔS° can be calculated from the slope and intercept. The results were listed in Table 6. The negative values of ΔG° and ΔH° for the two azo dyes indicated that the adsorption processes on the microparticles prepared from the A-method were spontaneous and exothermic. In addition, the positive values of ΔS° indicated the increased randomness during the adsorptions of two azo dyes on the microparticles. This might be attributed to liberation of water molecules from the hydrated shells of the sorbed species [27].

The pseudo-second-order rate constant of dye adsorption is expressed as a function of temperature by Arrhenius relationship using the Eq. (11) [13]:

$$\ln k_2 = \ln A - \frac{E_a}{RT} \quad (11)$$

The value of E_a can be calculated from the slope of a plot of $\ln k_2$ versus $1/T$. The magnitude of the activation energy (E_a) can give an idea about the type of adsorption which is mainly physical or chemical. The physisorption process usually has the activation energy (E_a) in the range of 5–40 kJ/mol, while the activation energy (E_a) in the range of 40–800 kJ/mol suggests the chemisorption process [30]. The values of activation energy (E_a) for the two dyes, 78.21 kJ/mol (RB5) and 173.85 kJ/mol (3R), both confirmed that the adsorptions of these dyes on the A-method microparticles were predominant on the chemisorption process (Table 6). The results corresponded well with those from the Dubinin-Radushkevich isotherm.

Table 6
The thermodynamic parameters and activation energies for adsorption of RB5 and 3R dyes on the A-method microparticles (diameter: 149–250 μm) at pH 3.0.

Parameter	K_L (S.D.) (L/mmol)	ΔG° (S.D.) (kJ/mol)	ΔH° (S.D.) (kJ/mol)	ΔS° (S.D.) (J/mol K)	E_a (S.D.) (kJ/mol)
RB5, T (°C)					
30	45.32 (2.07)	−27.20 (0.19)			
40	42.79 (0.15)	−27.53 (0.01)	−14.62 (2.86)	41.24 (5.09)	78.21 (3.10)
50	31.52 (0.77)	−28.04 (0.02)			
3R, T (°C)					
30	68.93 (7.66)	−28.18 (0.28)			
40	64.28 (4.08)	−28.77 (0.14)	−6.43 (1.29)	71.37 (6.48)	173.85 (1.40)
50	57.36 (3.39)	−29.41 (0.17)			

Note: S.D. in the parentheses is the standard deviation.

3.7. Competitive adsorption

Assuming there is no interaction between the two dyes (RB5 and 3R), the total absorbance for a mixture dye solution is equal to the summation of the absorbance of each dye, represented by Eq. (12). The adsorption capacity of each dye in a mixture solution can be calculated using the Eqs. (13) and (14):

$$A_\lambda = A_{RB5} + A_{3R} \quad (12)$$

$$A_{\lambda 1} = \varepsilon_{1RB5} L C_{RB5} + \varepsilon_{13R} L C_{3R} \quad (13)$$

$$A_{\lambda 2} = \varepsilon_{2RB5} L C_{RB5} + \varepsilon_{23R} L C_{3R} \quad (14)$$

The wavelengths of maximum absorbance for RB5 and 3R are at 597 (λ_1) and 494 (λ_2) nm, respectively. The concentrations of C_{RB5} and C_{3R} are calculated from the Eqs. (13) and (14). Hence the adsorption capacity of each dye in the mixture solution can be obtained.

The kinetics of the competitive adsorption in the mixture solution of the RB5 and 3R dyes on the A-method microparticles, with 2.0 mM initial concentration of each dye at pH 3.0 and 30 °C, were shown in Fig. 12. In Fig. 12(a), we can see that the initial adsorption rate of the 3R dye on the microparticles was slightly faster than that of RB5 dye. Moreover, the time it took for the 3R dye to reach the adsorption equilibrium was shorter than that for the RB5 dye. It might be caused by the difference between the molecular sizes of the two anionic dyes. The 3R dye is smaller than the RB5 dye and can thus diffuse easily into the microparticles than the RB5 dye [21]. Fig. 12(b) showed the curves for the ratio for adsorption capacity of each dye between the mixture solution of two dyes and in each single solution with the same initial concentration of each dye with time. The ratio of RB5 dye indicated to be remained almost 80%, while the ratio of 3R dye appeared to be less than 40%. It was apparent that the adsorption of the 3R dye on the microparticles in the mixture solution was much more affected by the existence of the RB5 dye than the other way around in the competitive adsorption.

3.8. Desorption and reuse

The capacities of the A-method microparticles for the RB5 and 3R dyes in the adsorption, desorption, and adsorption steps were shown in Fig. 13. As can be seen, the adsorption condition was at 2.0 mg/mL initial dye concentration, pH 1.0, and 30 °C. The desorption condition was at pH 12.0 of sodium hydroxide solution and 30 °C. At the first adsorption step for 24 h, the adsorption capacities for the RB5 and 3R dyes reached the values of 1884 and 1844 mg/g, respectively. After the desorption step for 24 h, the adsorbed RB5 and 3R dyes were removed about 58 and 31%, respectively, by sodium hydroxide solution at pH 12.0. This could be ascribed to the fact that, in the basic solution, the positively charged amino groups were deprotonated and the electrostatic interaction between chitosan and dye molecules became much weaker [14]. The second adsorption step revealed the similar dynamical shape of the first adsorption step. It can also be seen that the total adsorption capacities of the RB5 and 3R dyes are the same as those for the first adsorption step. Therefore, the microparticles can be reused for further dye adsorption.

4. Conclusion

The crosslinked chitosan prepared through the homogeneous coupling reaction and the microparticle formation from sodium hydroxide solution showed the largest adsorbed amounts toward the RB5 and 3R dyes than those from the three other methods through heterogeneous coupling reaction and microparticle formation using sodium hydroxide or sodium tripolyphosphate solutions. The dynamical experimental study was measured to investigate the dye adsorption mechanism on the microparticles. It was found that the dye adsorption accurately followed the second-order adsorption process. At the same time, the respective negative values of ΔG° and ΔH° for the RB5 and 3R dyes indicated that the adsorption process on the microparticles was spontaneous and exothermic. The experimental isotherm data were analyzed using three isotherm models, and the results revealed that the adsorption behaviors of the RB5 and 3R dyes on the crosslinked chitosan microparticles fitted well with the Langmuir model. In addition, the mean adsorption energy (E) from the Dubinnin-Radushkevich isotherm and the activation energy (E_a) from Arrhenius equation indicated that the adsorption process might be the dual nature of the process, physisorption and chemisorption, and was predominant on the chemisorption process of these dyes on the microparticles. The competitive adsorption showed that the adsorption of the 3R dye on the microparticles in the mixture solution was much more affected by the existence of the RB5 dye than the other way around. Furthermore, the crosslinked chitosan microparticles can be regenerated through the desorption of the dye in pH 12.0 of sodium hydroxide solution and can then be reused to adsorb the dye.

References

[1] G. Crini, Recent developments in polysaccharide-based materials used as adsorbents in wastewater treatment, Prog. Polym. Sci. 30 (2005) 38–70.
[2] Y.M. Slokar, A.M. Le Marechal, Methods of decolorization of textile wastewaters, Dyes Pigments 37 (1998) 335–356.
[3] I.T. Peternel, N. Koprivanac, A.M.L. Bozic, H.M. Kusic, Comparative study of UV/TiO_2, UV/ZnO and photo-Fenton processes for the organic reactive dye degradation in aqueous solution, J. Hazard. Mater. 148 (2007) 477–484.
[4] G. Crini, P.M. Badot, Application of chitosan, a natural aminopolysaccharide, for dye removal from aqueous solutions by adsorption processes using bath studies: a review of recent literature, Prog. Polym. Sci. 33 (2008) 399–447.
[5] E. Guibal, L. Dambies, C. Milot, J. Roussy, Influence of polymer structural parameters and experimental conditions on metal anion sorption by chitosan, Polym. Int. 48 (1999) 671–680.
[6] H. Yoshida, S. Fukuda, A. Okamoto, T. Ktaoka, Recovery of direct dye and acid dye by adsorption on chitosan fiber-equilibria, Water Sci. Tech. 23 (1991) 1667–1676.

[7] F.C. Wu, R.L. Tseng, R.S. Juang, Comparative adsorption of metal and dye on flake- and bead-types of chitosan prepared from fishery wastes, J. Hazard. Mater. B73 (2000) 63–75.
[8] F.C. Wu, R.L. Tseng, R.S. Juang, Enhanced abilities of highly swollen chitosan beads for color removal and tyrosinase immobilization, J. Hazard. Mater. B81 (2001) 167–177.
[9] S. Chatterjee, S. Chatterjee, B.P. Chatterjee, A.R. Das, Adsorption of a model anionic dye, ecosin Y, from aqueous solution by chitosan hydrobeads, J. Colloid Interface Sci. 288 (2005) 30–35.
[10] Z.G. Hu, J. Zhang, W.L. Chan, Y.S. Szeto, The sorption of acid dye onto chitosan nanoparticles, Polymer 47 (2006) 5838–5842.
[11] W.L. Du, Z.R. Xu, X.Y. Han, Y.L. Xu, Z.G. Miao, Preparation, characterization and adsorption properties of chitosan nanoparticles for eosin Y as a model anionic dye, J. Hazard. Mater. 153 (2008) 152–156.
[12] M.S. Chiou, H.Y. Li, Equilibrium and kinetic modeling of adsorption of reactive dye on crosslinked chitosan beads, J. Hazard. Mater. B93 (2002) 233–248.
[13] M.S. Chiou, H.Y. Li, Adsorption behavior of reactive dye in aqueous solution on chemical cross-linked chitosan beads, Chemosphere 50 (2003) 1095–1105.
[14] A.R. Cestari, E.F.S. Vieira, A.G.P. dos Santo, J.A. Mota, Adsorption of anionic dyes on chitosan beads. 1. The influence of the chemical structures of dyes and temperature on the adsorption kinetics, J. Colloid Interface Sci. 280 (2004) 380–386.
[15] M.S. Chiou, P.Y. Ho, H.Y. Li, Adsorption of anionic dyes in acid solutions using chemically cross-linked chitosan beads, Dyes Pigments 60 (2004) 69–84.
[16] M.S. Chiou, G.S. Chuang, Competitive adsorption of dye metanil yellow and RB15 in acid solution on chemically cross-linked chitosan beads, Chemosphere 62 (2006) 731–740.
[17] S. Rosa, M.C.M. Laranjeira, H.G. Riela, V.T. Favere, Cross-linked quaternary chitosan as an adsorbent for the removal of the reactive dye from aqueous solutions, J. Hazard. Mater. 155 (2008) 253–260.
[18] F.L. Mi, S.S. Shyu, S.T. Lee, T.B. Wong, Kinetic study of chitosan-tripolyphosphate complex reaction and acid-resistive properties of chitosan-tripolyphosphate gel beads prepared by in-liquid curing method, J. Polym. Sci. B: Polym. Phys. 37 (1999) 1551–1564.
[19] R.M. Silverstein, F.X. Webster, D.J. Kiemle, Spectrometric Identification of Organic Compounds, 7th ed., John Wiley & Sons, New York, NY, USA, 2005, pp. 72–126.
[20] H. Yoshida, A. Okamoto, T. Kataoka, Adsorption of acid dye on crosslinked chitosan fibers: equilibria, Chem. Eng. J. 48 (1993) 2267–2272.
[21] K. Vijayaraghavan, Y.S. Yun, Biosorption of C.I. Reactive Black 5 from aqueous solution using acid-treated biomass of brown seaweed Laminaria sp., Dyes Pigments 76 (2008) 726–732.
[22] I. Langumuir, The adsorption of gases on plane surfaces of glass, mica and platinum, J. Am. Chem. Soc. 40 (1918) 1361–1403.
[23] H.M.F. Freundlich, Over the adsorption in solution, Z. Physik. Chem. A57 (1906) 358–471.
[24] S.P. Ramnani, S. Sabharwal, Adsorption behavior of Cr(VI) onto radiation crosslinked chitosan and its possible application for the treatment of wastewater containing Cr(VI), React. Funct. Polym. 66 (2006) 902–909.
[25] A.H. Chen, S.C. Liu, C.Y. Chen, C.Y. Chen, Comparative adsorption of Cu(II), Zn(II), and Pb(II) ions in aqueous solution on the crosslinked chitosan with epichlorohydrin, J. Hazard. Mater. 154 (2008) 184–191.
[26] A.H. Chen, C.Y. Yang, C.Y. Chen, C.Y. Chen, C.W. Chen, The chemically crosslinked metal-complexed chitosans for comparative adsorptions of Cu(II), Zn(II), Ni(II) and Pb(II) ions in aqueous medium, J. Hazard. Mater. 163 (2009) 1068–1075.
[27] K.Z. Elwakeel, Removal of Reactive Black 5 from aqueous solutions using magnetic chitosan resins, J. Hazard. Mater. (2009), doi:10.1016/j.jhazmat.2009.01.051.
[28] J. Tellinghuisen, Van't Hoff analysis of K^0 (T): how good or bad? Biophys. Chem. 120 (2006) 114–120.
[29] A.M. Donia, A.A. Atia, K.Z. Elwakeel, Selective separation of mercury(II) using magnetic chitosan resin modified with Schiff's base derived from thiourea and glutaldehyde, J. Hazard. Mater. 151 (2008) 372–379.
[30] B.H. Hameed, A.A. Ahmad, N. Aziz, Isotherms, kinetics and thermodynamics of acid dye adsorption on activated palm ash, Chem. Eng. J. 133 (2007) 195–203.